

Numerical simulations of two-phase flow in photobioreactors

*Giovanni Luzi¹⁾, Christopher McHardy²⁾, Christoph Lindenberg³⁾,
Cornelia Rauh^{1,2,4)}, Antonio Delgado^{1,4)}

¹⁾ LSTME Busan Branch, Busan 46742, Republic of Korea

²⁾ Technische Universität Berlin, Fachgebiet Lebensmittelbiotechnologie und -
prozesstechnik, Königin-Luise Str. 22, 14195 Berlin, Germany

³⁾ OTH Amberg-Weiden, Department of Mechanical Engineering and Environmental
Engineering, Kaiser-Wilhelm-Ring 3, 92241 Amberg, Germany

⁴⁾ Friedrich-Alexander Universität Erlangen-Nürnberg, Lehrstuhl für
Strömungsmechanik, Cauerstraße 4, 91058 Erlangen, Germany

^{*)} giovanni.luzi@fau.de

ABSTRACT

The cultivation of phototropic microorganisms in photobioreactors (PBR) permit to achieve culture densities only in the order of few grams per litre. Consequently, harvesting and downstream processes turn out to be expensive. In order to investigate and maximize process conditions, multiphysics simulations of phototropic cell cultivation are regarded as a valid option compared to time consuming and expensive experiments. Nevertheless, such numerical simulations require a proper modelling of the fluid flow and the light field as well as the growth kinetics of algal cells. Recently, we compared two strategies for exposing cells to fluctuating light, namely pneumatic mixing and flashing light illumination, with respect to their ability to increase the productivity of a 5 cm diameter bubble column PBR at industrially relevant operating. We found, numerically, that the enhancement of pneumatic mixing does not affect the growth rate at all. In contrast, illumination with flashing LED leads to a significant increase of the growth rate if proper flashing frequencies are chosen.

So far, our numerical work has been conducted with commercial software which is usually costly and often does not allow much flexibility with respect to the possibility to modify the source code. In the present contribution, we focus on the CFD results obtained with OpenFOAM[®] and compare two models for the computation of the lift coefficient. OpenFOAM[®] is an open source software and it allows the end user to modify the built-in codes within an easy programming environment, so that light distribution and growth kinetic models can be included in the future.

1. INTRODUCTION

Processes involving multiphase flows are frequently encountered in reactor operations. Many different types of reactors exist and bubble columns are among the most used ones in industry. They are multiphase contactors and reactors which find applications in chemical, petrochemical and biological industries, only to cite a few. Their strength relies on design and maintenance simplicity, good heat and mass transfer properties, absence of sealing and mechanical moving parts associated with a low construction cost (Deckwer 1992). These characteristics makes them particularly appealing also for microalgae cultivation, since they provide the possibility to cultivate phototrophic organisms under low shear stress conditions. Multiphysics simulations are nowadays regarded as a powerful tool to investigate the complex physical phenomena occurring in PBR. In this context, the term “multiphysics simulation” is understood as the simultaneous simulation of independent physical phenomena, such as turbulent two-phase flows and light distribution. The modelling of gas-liquid two phase flow is rather complex and it has been the subject of intense studies during the last twenty years. It needs to be correctly computed since it affects gas liquid mass transfer, cell mixing and therefore growth conditions (Luzi 2019). Three-dimensional unsteady simulations are able to predict the complex flow patterns of a bubble column PBR with a reasonable degree of accuracy (Pfleger 1999) and (Pfleger 2001). Moreover, if all the interphase forces, i.e., drag, lift, virtual mass, wall lubrication and turbulent dispersion forces are incorporated in the simulations, numerical predictions significantly improve in comparison with experimental results. (Masood 2014) utilized the commercial software ANSYS CFX[®] to deeply analyse and compare different turbulent closure and drag force models. In addition, they extensively investigated the effect of different interphase force models on the flow field.

Recently, fluid flow in bubble columns have been simulated also with the open source software OpenFOAM[®]. (Weber 2017) simulated a pseudo 2D bubble column comparing the Euler-Lagrange with the Euler-Euler approach and experiments by using OpenFOAM[®]. Comparison of the bubble size distribution and gas hold-up with experimental outcomes shows a good accordance. (Asad 2017) combined the discrete bubble model (DBM) with the volume of fluid approach (VOF) to study the hydrodynamics of a rectangular bubble column, testing three different drag models. All the investigated drag models give predictions which compare favourably with the experimental results of Deen (2000), in terms of the time averaged vertical component of the liquid velocity and liquid velocity fluctuations, as well as the time averaged vertical component of the gas velocity. However, bubble dynamics and the instantaneous flow field showed notably differences. (Vieira 2018) also examined a rectangular bubble column reactor, considering coalescence and break-up phenomena by means of the Quadrature Method of Moments (QMOM). They also investigated three different RANS $k - \varepsilon$ models, namely the standard, the modified and the mixture variant. (Chen 2018) performed numerical simulations of two-phase flow in a bubble column taking into account coalescence and break up phenomena by means of a population balance equation (PBE). Their numerical findings agree well with experimental results in terms of time averaged vertical component of liquid velocity, gas hold up and turbulent energy dissipation rate.

In the present contribution, we utilise the open source software OpenFOAM® to simulate the two-phase fluid flow inside a PBR and we compare the results obtained with two different models of lift coefficient, i.e. the Legendre-Magnaudet and Tomiyama one. We find that the choice of the lift coefficient strongly affects the flow behavior in the reactor as well as the time averaged gas hold-up and the vertical component of the liquid velocity.

2. SIMULATION SET UP

2.1 Geometry and Grid

In this study, we consider a cylindrical PBR. The height is 50 [cm] and its diameter is 5 [cm]. The inlet sparger has a diameter of 1 [cm] and it is situated at the bottom base of the PBR. We utilize the mesh we have employed in our previous works, see McHardy (2018) and Luzi (2019). A detailed description can be found in McHardy (2018), and it will not be repeated here. Here, we only mention that both geometry and grid have been generated with ANSYS ICEM® and the domain is covered with a structured mesh made of 54802 cells.

2.2 Mathematical modelling of fluid flow

We employ the Euler-Euler formulation to simulate the two-phase flow, where individual bubbles are not considered and the dispersed phase is ensemble averaged. In this context, the mass conservation equation for both phases k read

$$(1) \quad \frac{\partial}{\partial t}(\rho_k \alpha_k) + \nabla \cdot (\rho_k \alpha_k \mathbf{u}_k) = 0.$$

Herein, \mathbf{u}_k , α_k and ρ_k are the velocity, volume fraction and density of each phase, respectively. In Eq. (1) $k = L, G$. L indicates the liquid and G the gas phase. In Eq. (1) we have neglected the interphase mass transfer. The momentum equations for both phases may be written as

$$(2) \quad \frac{\partial}{\partial t}(\rho_k \alpha_k \mathbf{u}_k) + \nabla \cdot (\rho_k \alpha_k \mathbf{u}_k \mathbf{u}_k) = \nabla \cdot (\alpha_k \boldsymbol{\tau}_k) - \alpha_k \nabla p + \rho_k \alpha_k \mathbf{g} + \mathbf{M}_{s,k},$$

where $k = L, G$ and $s = L, G$ too. The left-hand side of Eq. (2) includes the temporal and the inertial convective acceleration of each phase. The right-hand side of Eq. (2) contains the divergence of the viscous stress tensor of each phase, the pressure gradient, the gravity and interphase forces. The stress tensor reads

$$(3) \quad \boldsymbol{\tau}_k = \mu_{k,eff} \left[\nabla \mathbf{u}_k + (\nabla \mathbf{u}_k)^T - \frac{2}{3} \mathbf{I}(\nabla \cdot \mathbf{u}_k) \right].$$

Herein, the effective dynamic viscosity $\mu_{k,eff}$ is the sum of the molecular and the turbulent viscosity, i.e.

$$\mu_{k,eff} = \mu_{k,Lam} + \mu_{k,Turb}.$$

(4)

Turbulence modelling is necessary in order to have results that qualitatively agree with experiments. (Pfleger 2001) contrasted experimental results with numerical simulations, comparing laminar and turbulent flow modelling. As far as the time averaged vertical component of the liquid velocity concerns, the laminar model overestimates the fluid velocity in many points. For instance, the velocity at the centreline of the reactor has almost a doubled value compared to experiments. In addition, the trend of the velocity profile over time indicates much smaller peaks compared to experimental results.

The last term $M_{s,k}$ in Eq. (2) represents the averaged interphase forces. It incorporates the contribution of the drag, lift, virtual mass, wall lubrication and turbulent dispersion forces. In our simulations, we utilize the Ishii-Zuber correlation (Ishii 1979) to evaluate the drag coefficient C_D . This drag model distinguishes three bubble regimes, i.e. the spherical bubble, the ellipse distorted and the cap distorted regime, for more details, see Ishii (1979). In case of the lift force, we employ the Legendre-Magnaudet and the Tomiyama model (Tomiyama 2002) to compute the lift force coefficient C_L . The former reads (Legendre 1998)

$$C_L = \sqrt{(C_{L,LowRe})^2 + (C_{L,HighRe})^2},$$

(5)

while the latter may be written as (Frank 2004)

$$C_L = \begin{cases} \min[0.288 \tanh(0.121 Re_p, f(Eo'))], & Eo' < 4 \\ f(Eo'), & 4 \leq Eo' \leq 10 \\ -0.27, & Eo' > 10 \end{cases}.$$

(6)

Herein, $f(Eo') = 0.00105Eo'^3 - 0.0159Eo'^2 - 0.0204Eo' + 0.474$ and Eo' is a modified Eötvös number based on the long axis of a deformable bubble.

The virtual mass force accounts for the additional mass a gas bubble possesses by dragging an amount of liquid during its motion inside the PBR. We use a fixed value of the virtual mass coefficient, i.e. $C_{VM} = 0.5$.

Finally, we utilize the Frank model to calculate the wall lubrication force coefficient $C_{WL} = 0.5$, see Frank (2004) and Frank (2008), and the Favre averaged model (Burns 2004) to compute the turbulent dispersion forces.

2.3 Turbulence modelling

In order to compute the turbulent eddy viscosity $\mu_{k,Turb}$ we employ the mixture $k - \varepsilon$ model for both phases (Bezhadi 2004). The equation for k_m reads:

$$\frac{\partial}{\partial t}(\rho_m k_m) + \nabla \cdot (\rho_m k_m \tilde{\mathbf{u}}_m) = \nabla \cdot \frac{\mu_m^t}{\sigma_m} \nabla k_m + P_k^m - \rho_m \varepsilon_m + S_k^m, \quad (7)$$

while the one for ε_m is

$$\frac{\partial}{\partial t}(\rho_m \varepsilon_m) + \nabla \cdot (\rho_m \varepsilon_m \tilde{\mathbf{u}}_m) = \nabla \cdot \frac{\mu_m^t}{\sigma_m} \nabla \varepsilon_m + \frac{\varepsilon_m}{k_m} (C_{\varepsilon 1} P_k^m - C_{\varepsilon 2} \rho_m \varepsilon_m) + C_{\varepsilon 3} \frac{\varepsilon_m}{k_m} S_k^m. \quad (8)$$

Both k_m and ε_m are related to the corresponding variables of the continuous phase via the following relationships

$$k_m = \left(\bar{\alpha}_L \frac{\rho_L}{\rho_m} + \bar{\alpha}_G \frac{\rho_G}{\rho_m} C_t^2 \right) k_L, \quad (9)$$

and

$$\varepsilon_m = \left(\bar{\alpha}_L \frac{\rho_L}{\rho_m} + \bar{\alpha}_G \frac{\rho_G}{\rho_m} C_t^2 \right) \varepsilon_L. \quad (10)$$

In turn, k_L and ε_L are related to the corresponding variables for the disperse phase via

$$k_G = C_t^2 k_L, \quad (11)$$

and

$$\varepsilon_G = C_t^2 \varepsilon_L, \quad (12)$$

for more details about the model, see Bezhadi (2004).

2.4 Simulation details

In this section we report the main settings and boundary conditions used in the simulations. At the inlet sparger location, we set a fixed value of the air mass flow rate. At the outlet location on top of the PBR, we select the option *pressureInletOutletvelocity* for the velocity field, and *InletOutlet* for k , ε , k_m and ε_m .

The *pressureInletOutletvelocity* boundary condition specifies a zero gradient for the velocity in case of outflow. In case of inflow, a velocity value is assigned based on the flow rate. The *InletOutlet* boundary condition is equivalent to a zero gradient one, but in case of backflow a value is assigned to a specific field. At the walls, we impose a no-slip boundary condition for the velocity of both fluids, a zero gradient for k_m and ε_m , and the wall functions *kqRWallFunction* and *epsilonWallFunction* for k and ε , respectively. The height of the air headspace on the upper part of the reactor is 10 [cm].

The mean bubble diameter is set constant to $d_b = 7$ [mm] and the value of the gas superficial velocity used in the simulations is $u_G = 5$ [mm/s]. Gauss-based schemes have been utilized to discretize the gradient, divergence and Laplacian terms of the governing equations. We selected the Geometric-Algebraic Multi-Grid (GAMG) strategy in order to solve the pressure equation. We chose the Diagonal-based Incomplete Cholesky solver to reduce the residual up to a maximum value of 10^{-8} . To solve the equations of the velocity, k_m and ε_m , we utilize the *symGaussSeidel* solver with maximum value of the residual equal to 10^{-7} . We select the PIMPLE algorithm to link pressure and velocity. This algorithm combines the PISO and SIMPLE ones. The former is utilized for transient cases but it has severe limitations on the time step, while the latter is used for steady-state cases and it converges relatively fast, allowing also equations to be under-relaxed. The PIMPLE algorithm is based on the same formulation of the PISO one, but at each time step it can be thought to be as the SIMPLE one.

We set the under-relaxation factor equal to 0.8 for all the equations. We specify the number of *nCorrectors* and *nOuterCorrectors* equal to 2. The former is the number of times the pressure equation is solved, while the latter is the number of times the coupled system of equations is solved.

We choose the implicit Euler scheme to integrate the system of equations in time, together with an adaptive time step based on the maximum value of the Courant number and the maximum value of Δt . We set $\Delta t_{max} = 1$ [s] and we run the simulations up to $t = 300$ [s].

3. RESULTS AND DISCUSSION

During their motion towards the top of the reactor, gas bubbles form a meandering “plume” which is also termed as bubble column. It randomly oscillates within the PBR, moving the liquid phase which contains algae cells. This results in fast mixing times, which are approximately of 20 [s] for the common values of the gas superficial velocities utilized to operate PBR (Jung 2017). Due to the motion of the liquid phase, algae are continuously transported from regions of high to low light intensity and vice versa. Regions of high light intensity are located close to the PBR lateral surfaces, since they are in the vicinity of the light sources. On the contrary, low light intensity level areas are found to be close to the reactor center. The shuttling can potentially improve the photosynthetic efficiency, that is the number of photons utilized for building new biomass, see Luzi (2019) and Garcia Camacho (2003).

Both, Fig. 1 a) and b) show the contour of the air volume fraction at $t=142$ [s] on a x-y plane at $z=0$ [m]. Fig. 1a) depicts the results which were obtained by using the Legendre-Magnaudet model to compute C_L . Fig. 1b) illustrates the outcomes in case that the Tomiyama model has been employed to calculate the lift coefficient. Results obtained with both models show an oscillating column formed by gas bubbles during their upward motion in a PBR. Qualitative observations immediately denote a difference between the results. In case of the Legendre-Magnaudet model, the plume evenly spread across the cross section of the PBR after a short distance from the inlet. In case of the Tomiyama model, gas bubbles have the tendency to remain concentrated close to the central axis of the PBR, even at heights in the vicinity of the gas-liquid interface

far away from the inlet sparger, see Fig. 1 b). These qualitative observations can be explained by analysing the time averaged air volume fraction.

Fig. 2 a) and b) compare the time averaged air volume fraction computed with the two models at two heights, i.e. at $y=0.05$ [m] and at $y=0.2$ [m]. In the vicinity of the inlet at $y=0.05$ [m], the profiles calculated with both models reach a peak in the proximity of the reactor centre and rapidly decay toward the PBR walls. Close to the top, the Legendre-Magnaudet model predicts a flattened profile over a large part of the PBR cross-section, forming two peaks in the proximity of the walls. Instead, the profile computed with the Tomiyama correlation again shows a well-defined peak in the centre. The air volume fraction approaches zero at the walls, since bubbles do not get in contact with the reactor surfaces but they only move near to them. This phenomenon is also experimentally observed: during the upward motion of the bubble column, the gas phase concentrates in regions near to the wall. It is correctly modelled by the wall lubrication forces, which enforce bubbles away from solid surfaces. The time averaged air volume fraction always reaches a peak close to the main axis of the reactor and a rapidly decays towards the lateral surfaces, if the lift coefficient is computed with the Tomiyama model. This happens because in the Tomiyama model the lift coefficient changes sign if the sphere-volume equivalent diameter of a bubble exceeds the threshold value of 5.8 [mm], (Tomiyama 2002). Since in the simulations we set $d_B = 7$ [mm], bubbles are pushed toward the centre of the PBR by the reversal lift force during their upward motion. Differently, bubbles tend to depart from the centre of the reactor and approach the lateral surfaces of the PBR if the Legendre-Magnaudet model is used to calculate C_L . This results in a gas phase distribution, which is evenly spread across the reactor cross-section, already at heights close to the inlet sparger.

The distribution of the air volume fraction affects the time averaged velocity profile, see Fig. 3 a) and b). Numerical computations with both models predict an upward liquid flow close to the main axis of the reactor and a downward flow close to the walls. This trend is confirmed by the experimental and numerical results of Pflieger (1999). They performed LDA measurements of the time averaged vertical liquid velocity profile inside a cylindrical reactor. Close to the inlet sparger, the time averaged vertical component of the liquid velocity computed with the Tomiyama model exhibits a peak close to the PBR centre, which is narrower compared to the one computed with the Legendre-Magnaudet correlation, see Fig. 3 b). Approaching the walls, the profile of the time averaged vertical velocity computed with the Tomiyama model result flattened, while the Legendre-Magnaudet correlation predicts a steeper profile, and the values of the velocity are greater in magnitude compared to the Tomiyama case. On the top of the reactor, the magnitude of the time averaged vertical component of the liquid velocity reaches approximately similar values close to the walls. Moving towards the centre of the PBR, the Legendre-Magnaudet case exhibits a flattened profile over the cross-section of the reactor. In contrast, the Tomiyama case again shows a well-defined peak. Since the bubble column mainly moves the liquid phase, the peak of the vertical component of the liquid velocity in the centre of the reactor in case of the Tomiyama model is expected, since bubbles tend to remain more concentrated close to the main axis. By using the Legendre-Magnaudet correlation, bubbles are likely to disperse in the column, which also results in an evenly distributed velocity profile.

In the present work we have utilized a fixed value of the bubble diameter based

on some preliminary experiments. Specifically, we have recorded images with a high speed camera and we have used the Hough transform implemented in Matlab[®] to detect bubble shapes and compute a mean diameter. In future works, a more accurate experimental investigation will be carried out in order to determine bubble sizes. This will be crucial for numerical computations, especially if a mean bubble diameter results greater than 5.8 [mm], since the lift force in Tomiyama reverses its sign. On the contrary, if the mean bubble diameter is smaller than 5.8 [mm], significant deviations between the results obtained with the Tomiyama and Legendre-Magnaudet model should not be expected. (Masood 2015) compared his numerical results with the experiments of Deen (2000) for the case of a squared bubble column operated at $u_G = 4.9$ [mm/s], and keeping $d_B = 4$ [mm]. Specifically, they compared the time averaged vertical component of the liquid and gas velocity profiles at different heights inside the reactor. They also used the Ishii-Zuber correlation for the drag force and four different lift models to calculate C_L , i.e. a constant value, Tomiyama, Legendre-Magnaudet and Saffmann models. The time averaged velocity profiles show similar trends, if C_L is computed with the Tomiyama model and Legendre-Magnaudet correlation, which differs significantly from our findings. This is probably due to the size of the mean bubble diameter used in the simulation, as discussed previously. In addition, in our experiments we always observed smaller bubbles close to the lateral surfaces of the reactor and bigger bubbles closer to the centre. Our experimental

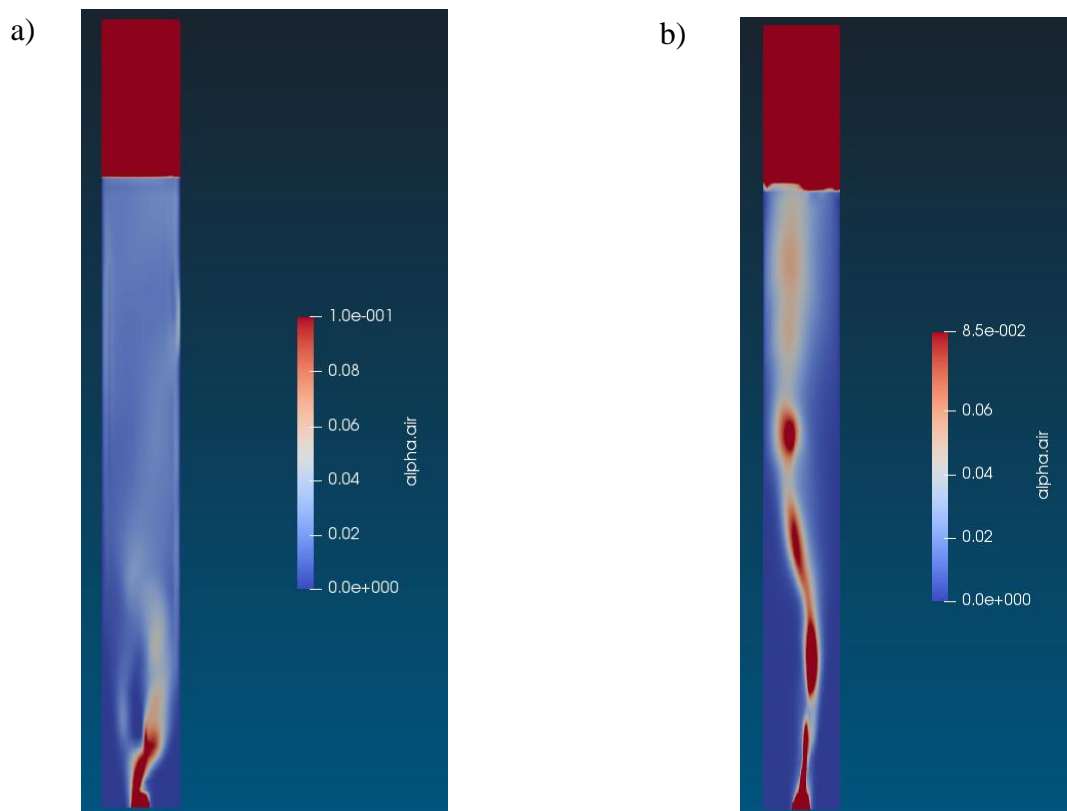


Fig. 1 Air volume fraction on an x-y plane at $z=0$ at $t=142$ [s]. The lift force coefficient C_L has been computed with the Legendre-Magnaudet model a) and with the Tomiyama correlation b). The gas superficial velocity is 5 [mm/s].

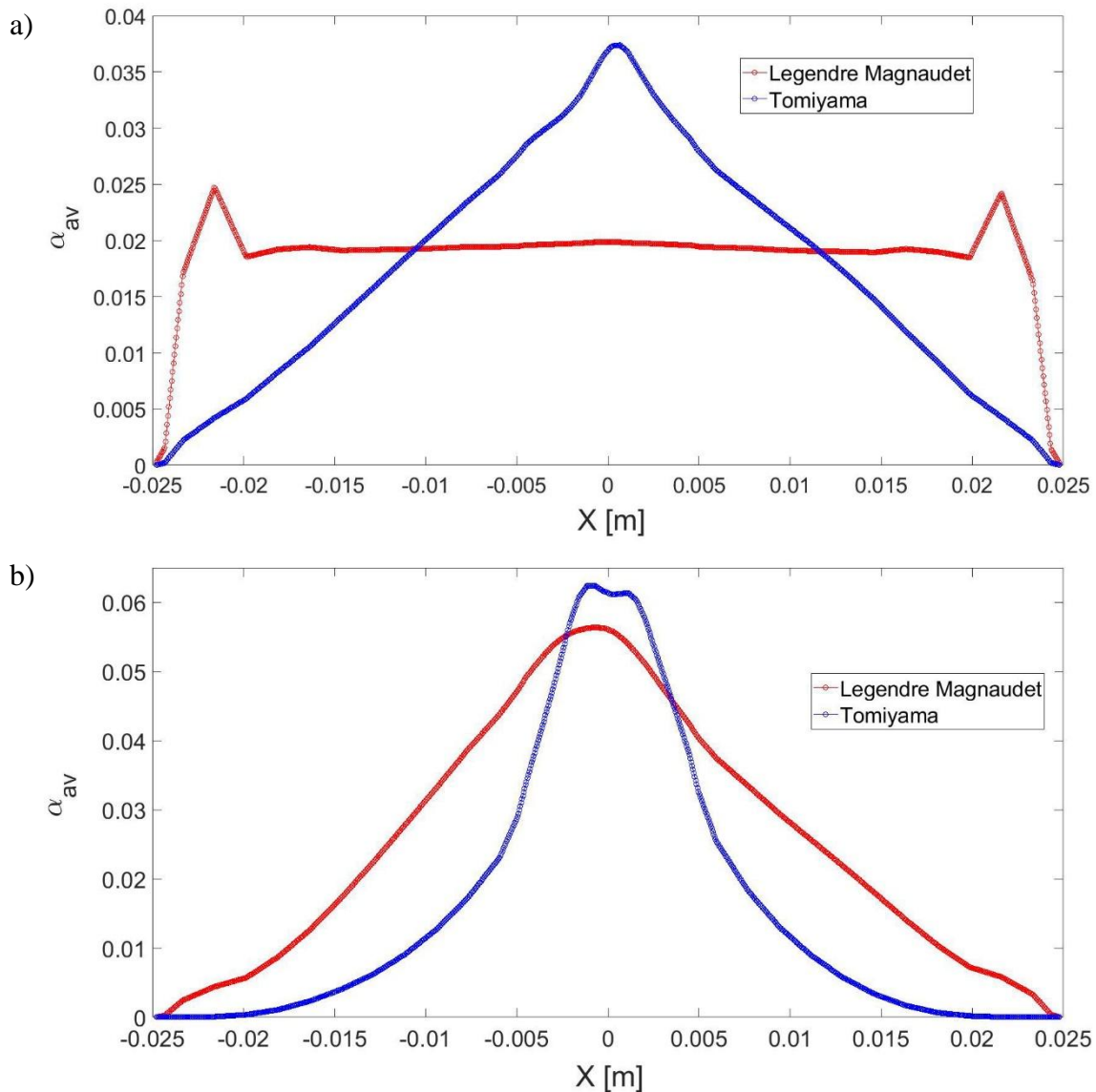


Fig. 2 Time averaged air volume fraction on a x-y plane at $z=0$ at $y=0.2$ [m] a) and $y=0.05$ [m] b). The lift coefficient C_L has been computed with two different correlations: Legendre-Magnaudet (red line) and Tomiyama (blue line). The gas superficial velocity is 5 [mm/s].

findings are in agreement with those of Buwa (2002). In order to obtain a more homogeneous bubble size distribution, a different sparger can be used. In preliminary experiments with a ring sparger, we have observed a more uniform bubble size distribution compared to a dip-tube sparger. This could potentially improve the agreement between experiments and simulations, if a mean diameter is used in numerical computations. As an alternative, a bubble population balance equation (BPBE) could be implemented in order to consider a bubble size distribution. However,

the numerical study of Chen (2005) clearly indicates that the time averaged vertical component of the liquid velocity profiles are very similar with or without the implementation of a (BPBE) in the bubbly flow regime. On the contrary, they obtained a better agreement between numerical and experimental data by using BPBEs in the churn-turbulent flow regime, where coalescence and breakup phenomena are important.

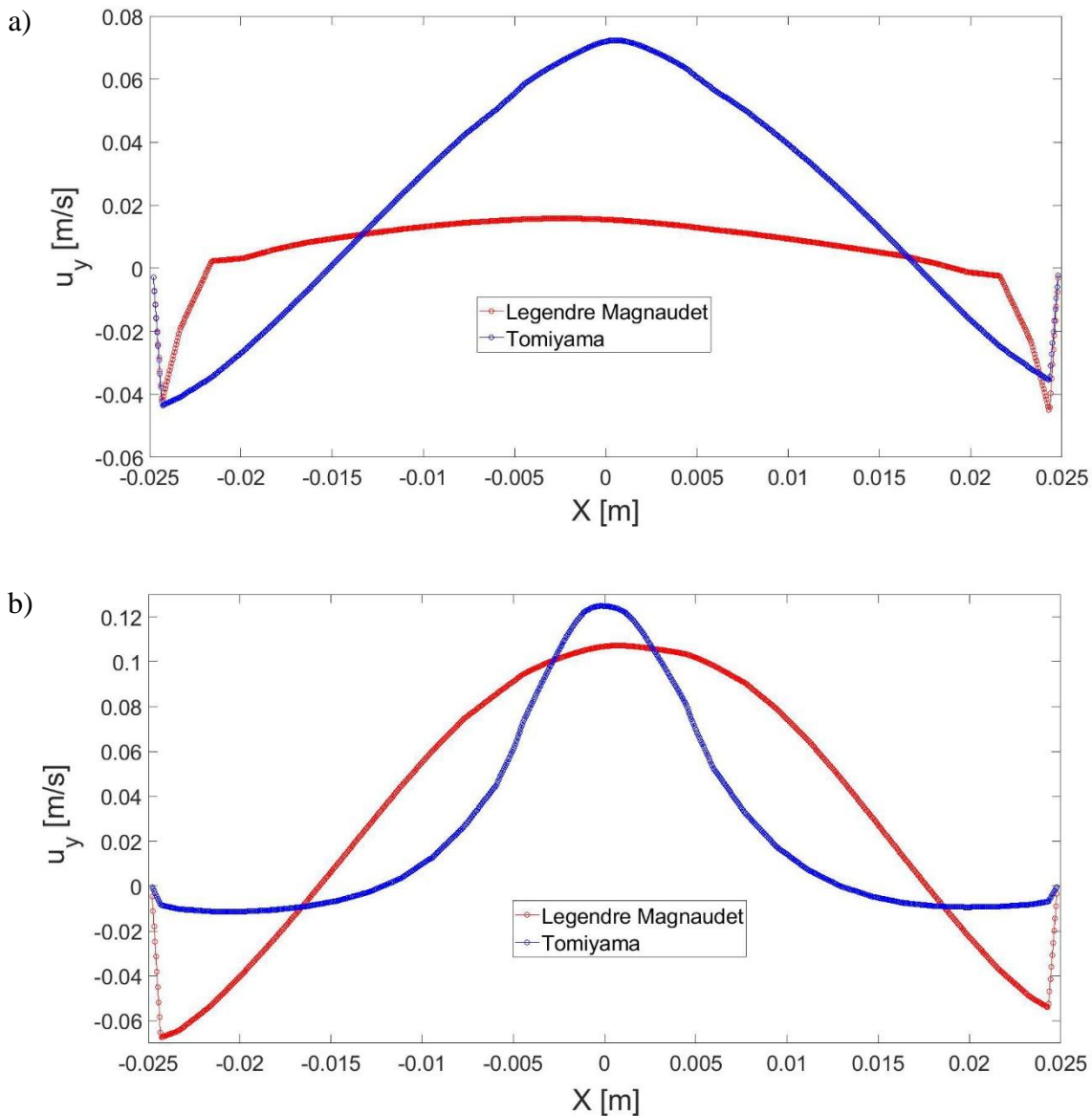


Fig. 3 Time averaged vertical component of the liquid velocity on a x-y plane at $z=0$ at $y=0.2$ [m] a) and $y=0.05$ [m] b). The lift coefficient C_L has been computed with two different correlations: Legendre-Magnaudet (red line) and Tomiyama (blue line). The gas superficial velocity is 5 [mm/s].

4. CONCLUSIONS

In this work we performed numerical simulations of the two-phase fluid flow in a PBR. Specifically, we compared the results obtained by using two different correlations for the lift coefficient C_L , i.e. the Legendre-Magnaudet and the Tomiyama one. We analysed the case of the gas superficial velocity $u_g = 5$ [mm/s]. Numerical results show an irregular motion of the bubble plume in both cases. However, the trend of the time averaged air volume fraction and vertical liquid velocity profile at different heights inside the reactor exhibit significant differences. Discrepancies are due to the fact that the Tomiyama model predicts a change of the sign of the lift coefficient if the sphere-volume equivalent diameter of a bubble exceeds a threshold value.

REFERENCES

- Asad, A., Kratzsch, C., Schwarze, R. (2017), "Influence of drag closures and inlet conditions on bubble dynamics and flow behavior inside a bubble column", *Eng. Appl. Comput. Fluid Mech.* **11**(1), 127–141.
- Behzadi, A., Issa, R.I., Rusche, H. (2004), "Modelling of dispersed bubble and droplet flow at high phase fractions", *Chem. Eng. Sci.* **59**(4), 759–770.
- Braga Vieira, C., Litrico, G., Askari, E., Lemieux, G., Proulx, P. (2018), "Hydrodynamics of Bubble Columns: Turbulence and Population Balance Model", *ChemEngineering* **2**(12), 1–26.
- Bhusare, V.H., Dhiman, M.K., Kalaga, D. V, Roy, S., Joshi, J.B. (2017), "CFD simulations of a bubble column with and without internals by using OpenFOAM", *Chem. Eng. J.* **317**(1), 157–174.
- Burns, A. D. B., Frank, Th., Hamill, I., Shi, J-M. (2004), "The Favre Averaged Drag Model for Turbulent Dispersion in Eulerian Multi-Phase Flows", *5th International Conference on Multiphase Flow*, Yokohama.
- Buwa, V. V, Ranade, V. V, (2002). "Dynamics of gas–liquid flow in a rectangular bubble column: experiments and single/multi-group CFD simulations", *Chem. Eng. Sci.* **57**(22-23), 4715–4736.
- Cheng, J., Li, Q., Yang, C., Zhang, Y., Mao, Z. (2018), "CFD-PBE simulation of a bubble column in OpenFOAM ☆", *Chinese J. Chem. Eng.* **26**(9), 1773–1784.
- Chen, P., Sanyal, J., Duduković, M. (2005), "Numerical simulation of bubble columns flows: Effect of different breakup and coalescence closures", *Chem. Eng. Sci.* **60**(4), 1085-1101.
- Deckwer, W.-D. and Field, R.W., (1992), *Bubble column reactors*, Wiley, Chichester, NY.
- Deen, N. G., Hjertager, B.H., Solberg, T. (2000), "Comparison of PIV and LDA Measurement Methods Applied to the Gas-Liquid Flow in a Bubble Column", *10th*

International Symposium on Application of Laser Techniques to Fluid Mechanics, Lisbon.

Frank, Th., Shi, J. M., Burns, A. D. (2004), "Validation of Eulerian Multiphase Flow Models for Nuclear Safety Applications", *3rd International Symposium on Two-Phase Flow Modelling and Experimentation*, Pisa.

Frank, Th., Zwart, P. J., Krepper, E., Prasser, H.-M., Lucas, D. (2008), "Validation of CFD models for mono- and polydisperse air-water two-phase flows in pipes", *J. Nuclear Engineering & Design*, **238**(3), 647–659.

García-Camacho, F., Sánchez-Mirón, A., Molina-Grima, E., Camacho-Rubio, F., Merchuck, J.C. (2012), "A mechanistic model of photosynthesis in microalgae including photoacclimation dynamics", *J. Theor. Biol.* **304**, 1–15.

Ishii, M. and Zuber, N. (1979), "Drag coefficient and relative velocity in bubbly, droplet or particulate flows", *AIChE J.* **25**(5), 843–855.

Jung, S., Hahm, J., Luzi, G., Buchholz, R., Lindenberger, C. (2017), "Prediction method of scale-dependent growth characteristics of *A. platensis*", *Theor. Appl. Chem. Eng.* **23**(2), 2505-2508.

Legendre, D., Magnaudet, J. (1998), "The lift force on a spherical bubble in a viscous linear shear flow", *J. Fluid Mech.*, **368**, 81-126.

Luzi, G., McHardy, C., Lindenberger, C., Rauh, C., Delgado, A. (2019), "Comparison between different strategies for the realization of flashing-light effects – Pneumatic mixing and flashing illumination", *Algal Res.* **38**, 101404.

Masood, R. M. A., Delgado A. (2014), "Numerical investigation of the interphase forces and turbulence closure in 3D square bubble columns", *Chem. Eng. Sci.*, **108**, 54-168.

Masood, R. M. A., Jovicic, V., Delgado. A. (2015), "Numerical Simulation of Interfacial Closures for 3D Bubble Column Flows", *Chem. Eng. Technol.* **38**(5), 777–86.

McHardy, C., Luzi, G., Lindenberger, C., Agudo, J.R., Delgado, A., Rauh, C. (2018), "Numerical analysis of the effects of air on light distribution in a bubble column photobioreactor", *Algal Res.* **31**, 311–325.

Pfleger, D., Gomes, S., Gilbert, N., Wagner, H.-G. (1999), "Hydrodynamic simulations of laboratory scale bubble columns fundamental studies of the Eulerian–Eulerian modelling approach", *Chem. Eng. Sci.* **54**(21), 5091–5099.

Pfleger D., Becker S. (2001), "Modelling and simulation of the dynamic flow behavior in a bubble column", *Chem. Eng. Sci.*, **56**(4), 569-582.

Tomiyama, A., Tamai, H., Zun, I., Hosokawa, S. (2002), "Transverse Migration of Single Bubbles in Simple Shear Flow", *Chem. Eng. Sci.* **57**(11), 1849-1858.

Weber, A., Bart, H.-J. (2018), "Flow Simulation in a 2D Bubble Column with the Euler-Lagrange and Euler-Euler Method", *Open Chem. Eng. J.* **12**, 1–13.